Mon. Not. R. astr. Soc. (1967) **135**, 99–119.

SPECTROPHOTOMETRY OF THE OBJECT η CARINAE

A. W. Rodgers and Leonard Searle

(Received 1966 June 1)

Summary

Results of observations of the object η Carinae obtained with the coudé spectrograph and photoelectric spectrophotometer at Mount Stromlo are presented. The spectrum of η Carinae is characterized by the well known strong emission line spectrum overlying a smooth continuum which contributes about 60% of the radiation of η Carinae in the range 3300–11 000 Å. An analysis of the forbidden lines of N II and S II and of the hydrogen radiation shows that 10^{49} cm^3 of the volume of η Carinae is at an electron temperature of 2×10^4 °K and an electron density of 3×10^6/cm^3. Hydrogen is collisionally ionized and the Balmer lines are subject to large self-absorption effects. Ephemeral lines of Ne II, Ar III and Fe III arise in a smaller volume with an electron temperature near 50 000° K. Nitrogen, sulphur and oxygen are underabundant in η Carinae relative to population I B stars. A mass of 0·025 $M_\odot$ is derived for the ionized hydrogen in η Carinae. Some of the difficulties associated with a synchrotron hypothesis for the origin of the optical continuum in η Carinae are discussed. The outburst of η Carinae involved energies of 10^{49} erg and a mass of about 0·2 $M_\odot$ showing noteworthy similarities to the Crab supernova explosion.

1. *Introduction.* We present in this paper the result of absolute spectrophotometry of the object η Carinae. Since the early nineteenth century, variations in the brightness of η Carinae have been the subject of extensive observations which have been summarized by Innes (1) and O'Connell (2). The main features of the light curve are, commencing from the positive observations of η Carinae by Halley, a slow irregular brightening from the fourth magnitude in 1677 to a maximum of about $-0{\cdot}5$ in 1843 followed by a relatively rapid decline to the eighth magnitude at the end of the nineteenth century and a further slow, irregular brightening to nearly the sixth magnitude in 1965. More rapid irregular fluctuations of up to a magnitude are superimposed on this general variation. It is worthwhile here to emphasize the difference between this light curve, the most prominent feature of which appears to be the major decline in brightness between 1843 and 1890, and those of typical novae or supernovae.

Spectroscopic observations of η Carinae have been obtained at intermittent intervals since 1889 and culminate in the extensive series of line identifications made by Thackeray (3, 4) and Gaviola (5). References to early spectroscopic observations are given by Merrill (6) in a paper in which he identifies a large proportion of the predominantly bright line spectrum of η Carinae with lines of [Fe II], the other stronger lines being identified with the Balmer series, Fe II, Ti II and Cr II. During the interval in which observations have been obtained, the spectrum of η Carinae has remained sensibly of the same kind, i.e. bright lined with some observers reporting deeply exposed plates as showing a continuum, weak compared with the emission line intensities. However, a notable exception occurred at the epoch of a secondary light maximum in 1893

when η Carinae showed a rich absorption line spectrum corresponding to that of an F5 supergiant with strong superimposed emission lines of H and Fe II.

More minor changes have occurred in the relative intensities of the emission lines. Thackeray (3) reported variations in the relative strengths of Fe II and Ti II lines as compared with those observed in 1919. Rapid and marked changes have also occurred; for a few months in 1948 Gaviola (4) found that the lines of He I, [Ne III], [Fe III] and [N II] faded out and returned in 1949 to their previous brightness. Our own spectroscopic observations show similar fading of the He I, [Ne III] and [Fe III] lines in the twelve months interval between 1964 March and 1965 March. Continuing observations to determine the time scale of these variations are important. The light time corresponding to the radius (taken here to be 2·5″ at 1500 pc) is about one month while the transit time at a velocity indicated by the widths and displacement of lines in the spectrum of η Carinae, taken to be mass motions of about 500 km/s, is about 30 years. A major difference between the line identifications made by Gaviola and Thackeray concerns the lines [O II], [O III] and O II. Their absence on Thackeray's 1951 and 1952 plates suggested to him that oxygen was deficient in η Carinae compared with the slow nova RR Telescopii while Gaviola, on plates obtained between 1944 and 1951, identified faint lines from these two ions.

The complex form of η Carinae can be seen in Gaviola's published photographs (7). His shortest exposures in good seeing (one second in duration) show a non-stellar image; deeper plates show Gaviola's aptly named homunculus having extensions to 5″ and surrounding it a fainter nebulosity detectable to 15″. The homunculus and its extensions are of irregular surface brightness. Individual bright regions (Gaviola's 'condensations') have persisted for several decades, and Gaviola has summarized the proper motion measures of those within the homunculus and finds that the condensations are expanding from the nucleus at the rate of 5″/century, consistent with them having been ejected at the primary light maximum of last century. Our own direct photographic observations consist of plates taken with the 74 in. reflector (22″/mm) and the 26 in. refractor (18″/mm). The shortest exposures confirm the non-stellar appearance of the nucleus of η Carinae. There appears to be a uniform distribution of light over an asymmetrical region with a characteristic diameter of 1·5″ while the stellar images are one half this size. We have made observations of the monochromatic light distribution in η Carinae using a photoelectric scanner under conditions of excellent seeing and have found that half the light falls within 2·5″ radius (in good agreement with Thackeray's (8) computation that Gaviola's isophote 3 includes 52% of the light).

A remarkable feature of the literature is that while the condensations whose relative positions were measured as components of a multiple star between 1915 and 1938, are now regarded as non-stellar condensations in the object η Carinae, the nucleus itself is still referred to as a star in spite of its non-stellar visual and photographic appearance.

Following Thackeray's discovery of polarization in the halo, detailed photoelectric measures of the polarization in η Carinae and surrounding stars have been made by Visvanathan (9). He found intrinsic polarization in the nucleus ($r < 3''$) of 4·2% increasing to 9·0% in the annulus (9″–22″). This polarization is independent of wavelength and has the position angle of the electric vector perpendicular to the length of the homunculus.

2. *Observations*

(*a*) *Spectroscopic.* During the observing seasons of 1964 and 1965 we made spectroscopic observations of the nuclear and halo regions of η Carinae. Spectra of the bright nucleus were generally obtained with the 32 in. camera of the coudé spectrograph of the 74 in. reflector at Mount Stromlo. Using Kodak baked IIa-O and 103a-F emulsions the spectrum was photographed with a variety of exposure times with dispersions of 6·7 and 10·2 Å/mm over the wavelength range 3200–6850 Å. Spectra of the nucleus showing the Hα line were also obtained with the 120 in. coudé camera at 1·8 Å/mm. Further exposures on the nucleus were made with the 10 in. camera of the coudé spectrograph while spectra of the outer portions were photographed with the 3 in. and 8·5 in. cameras of the Newtonian spectrograph attached to the 74 in. reflector. The longest exposures with the 32 in. camera were of four hours duration, enabling the continuum to be recorded at a photometrically suitable density. Photometric wedge calibration exposures were superimposed on each plate. Direct intensity microphotometry was carried out mainly on the 32 in. camera plates and the profiles and equivalent widths of lines of interest expressed in terms of the continuum.

(*b*) *Photoelectric spectrophotometry.* In order to place the spectroscopic observations described above on an absolute basis, η Carinae was observed with a photoelectric scanner attached to the cassegrain focus of the Mount Stromlo 50 in. reflector. The scanner is of recent construction and a brief description here of its salient features is appropriate. The optics are of the standard Fastie–Ebert form. The collimator-camera focal length is 36 in. which at f/18 gives a 2 in. beam size. The grating is a Bausch and Lomb replica with 600 lines per mm blazed in the second order at 3750 Å; the resultant dispersions are 9·1 Å/mm and 18·2 Å/mm in the second and first orders respectively. The grating is rotated at a choice of speeds given by a five speed gearbox through a worm and sector giving the grating constant angular velocity. Symmetrically opening slits and deckers define the entrance and exit focal planes. A beam splitter is incorporated in the collimator beam which feeds light through a choice of glass filters, *U*, *B*, *V* to a photomultiplier; this monitoring channel is used to give information on sky transparency and guiding irregularities. A further filter wheel in the camera beam houses filters used to reject overlapping orders of the grating spectrum. Field lenses are mounted in the cold boxes used and produce images of the 50 in. mirror of 3 mm diameter on the cathodes of the RCA 1P21 and 7102 photomultipliers used until now. An auxiliary shaft from the gearbox rotating at one Ångström unit per revolution when the grating is used in the second order, drives a counter displaying the wavelength at the centre of the exit slit. In measuring bright objects continuous scans are made; for fainter stars, point by point charge integration has been used. Deviations from linearity (Å/unit time) in the combination of grating and strip recorder drive have been determined to be less than 0·07%. The scanner was designed by Rodgers and built by Precision Engineering Pty. Ltd. of Sydney, Australia. The optics were made in the Mount Stromlo optical shop.

The absolute energy calibration of the objects measured has been made by reference to Oke's (**10**) list of spectrophotometric standards. Atmospheric extinction corrections were determined in the standard manner and the reductions made using the IBM 1620 computer of Mount Stromlo Observatory.

Scanner observations of η Carinae commenced in 1964 November. Measurements of the wavelength region 3300–5944 Å were made on five nights between 1964 November and 1965 March and of the region, 5560–11 000 Å on five nights between 1965 January and 1965 June. On each night, at least three scans were made, each scan extending from the blue to red wavelength limit and return. η Carinae as measured was defined by a 1·75 mm diameter entrance slit (17″ diameter at the focus of the 50 in). Exit slit widths were varied from 0·5 mm (4–5 Å in order II) to 1·75 mm (15·7 Å in order II) for the continuous scans.

3. *Results*

(*a*) *Continuum.* A feature of the deeply exposed spectra of η Carinae is that below the many emission lines there is a smooth continuum. At several wavelengths in this continuum broad absorption features are seen. These are the absorption components of the P Cygni-like hydrogen and neutral helium lines, the Ca II lines of H and K and the complex absorption feature near the D lines of Na I. It should be emphasized that the continuum and these absorption lines cannot be identified with any known type of stellar spectrum.

In 20 Å wide bands centred on the wavelengths between λ 3509 Å and λ 6800 Å listed in Table I, the continuum was identified on microphotometer tracings on our high dispersion spectra. The fraction of the light in these bands due to the continuum was determined and the appropriate corrections applied to the low resolution scans. At wavelengths below λ 3509 Å many weak emission lines mask the continuum so that only an upper limit to the intensity of the continuum could be determined. To the red of λ 6800 Å we had no spectra with which to compare the scanner tracings. However even with the lower resolution of the first order scans there appeared in many parts of the infra red spectrum regions

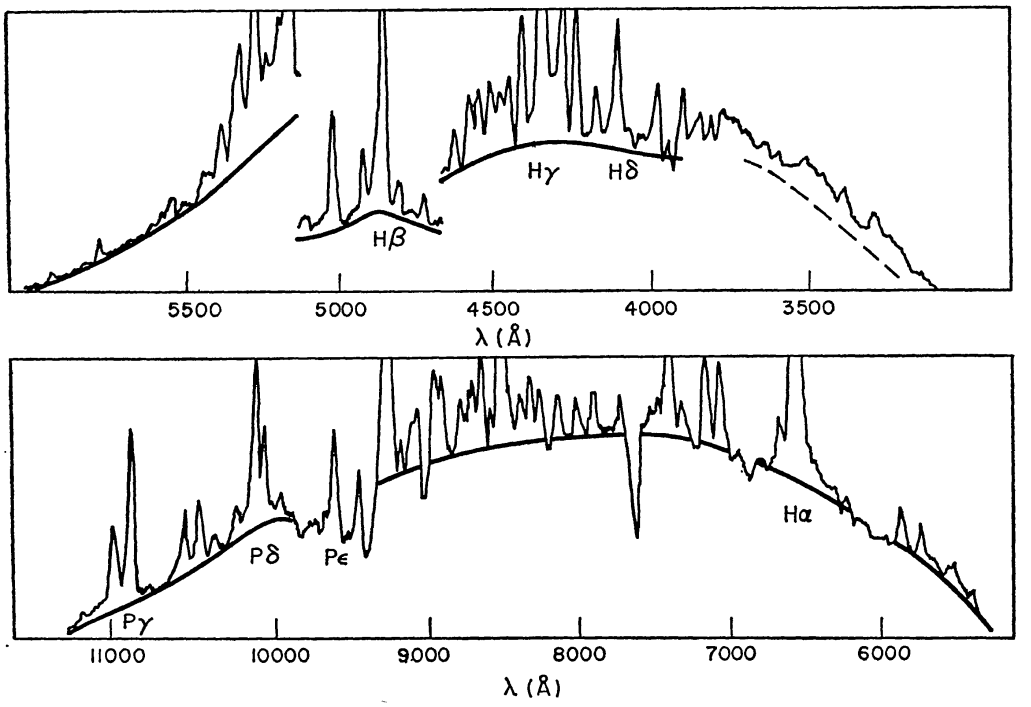

FIG. 1. *Copies of blue and infra-red scans of η Carinae. The scans illustrated were made with a 1·75 mm exit slit. The heavy line schematically shows the adopted continuum. It is broken at λ 4650 Å due to insertion of a filter and at λ 5200 Å due to an amplifier sensitivity change.*

which could plausibly be identified with a true continuum. Further obfuscation is due to the presence of telluric absorptions but we have been able to estimate their effect by reference to similar scans of early type stars. We show copies of the scanner tracings of η Carinae in Fig. 1 together with the position of the adopted continuum. Four regions between λ 5600 Å and λ 5900 Å were measured in common on the blue and infra-red scans and related to the scans of the spectrophotometric standards; in this manner the blue and infra-red scans were tied to each other.

The mean observed absolute energy distribution of the continuum of η Carinae is given in Table I. We show the relative fluxes in the form constant $-\log F_\nu$, where F_ν is the flux per unit frequency interval.

TABLE I

Mean observed continuum of η Carinae

λ(Å)	Constant $-\log F_\nu$	λ(Å)	Constant $-\log F_\nu$	λ(Å)	Constant $-\log F_\nu$
3390	2·02	5400	1·61	6065	1·50
3571	1·94	5500	1·60	6210	1·45
3654	1·89	5600b	1·54	6370	1·38
3930	1·94	5600r	1·52	6800	1·32
4082	1·92	5698b	1·42	7100	1·28
4189	1·90	5698r	1·51	7530	1·18
4598	1·82	5792	1·38	7850	1·14
4684	1·83	5800b	1·40	8000	1·13
4748	1·80	5800r	1·53	8400	1·05
4826	1·74	5842	1·54	8805	1·03
4979	1·70	5900b	1·48	9905	1·03
5000	1·71	5900r	1·52	10250	1·03
5100	1·72	5944	1·42	10400	1·01
5200	1·64	6000	1·52	10800	0·94
5300	1·62				

Note: b and r refer to wavelengths independently referred to standards observed with the blue and red cells.

By reference to Oke's standards and adopting Code's (11) value of of $3{\cdot}8 \times 10^{-9}$ erg/cm^2 s Å at λ 5560 Å for the flux of a star of $V=0$ we find the observed absolute flux of the η Carinae continuum, bounded by a 17″ aperture to be $1{\cdot}07 \times 10^{-11}$ erg/cm^2 s Å, corresponding to $V=6{\cdot}38$. This value can be compared with that of Feinstein (12) who measured the V magnitude of η Carinae in 1963 June as 6·22. Since Feinstein's measures include the flux from the emission lines, which contribute about 28% of the light in this wavelength region, we see that η Carinae has only slightly brightened in the last two years.

(*b*) *Reddening and absorption.* η Carinae lies in a region of bright nebulosity to which its name is often given. The region has a high surface density of OB stars and open clusters and is overlain by intense and irregular obscuration (13). Considerable evidence suggests that the OB stars extend in depth to distances of 5 kpc or more (14). The association of η Carinae with the nebulosity NGC 3372 and the O stars embedded in it has been discussed by Thackeray (15) and Gratton (16). Both authors favour the idea that η Carinae is involved

in the nebula and hence suffers similar interstellar absorption. Because of the irregularity of the obscuration in the vicinity of η Carinae we considered that the most reliable value of the interstellar reddening could be obtained by measurements of the hydrogen line intensities of the H II region as near to η Carinae as possible but where background stars or η Carinae itself could not affect the observations. To this end we intensively scanned a region 17″ in diameter, centred 20″ from η Carinae in position angle 250°. We found that the Paschen lines fell below the limiting brightness measurable with the 7102 cell and to compute the reddening we were forced to rely on a comparison of the observed and theoretical Balmer decrements. We assume that the unreddened decrement of the H II region is that computed by Burgess (**17**) for case B at an electron temperature of 10^4 °K. In Table II we compare the observed and computed decrements; we express the line intensities in the form $-2{\cdot}5 \log I$.

TABLE II

Comparison of observed and theoretical Balmer decrements in H II region near η Carinae

	$1/\lambda(\mu^{-1})$	Constant $-2{\cdot}5 \log I$ (Theoretical)	Constant $-2{\cdot}5 \log I$ (Observed)	Difference due to reddening (Magnitudes)
Hα	1·52	3·95	3·49	−0·46
Hβ	2·06	5·00	5·00	+0·00
Hγ	2·31	5·78	6·01	+0·23
Hδ	2·44	6·40	7·03	+0·63

The reddening found from Table II corresponds to $E_{B-V}=0{\cdot}69$. Feinstein (**12**) has derived photometric colour excesses of up to 0·50 for the surrounding stars of the cluster Trumpler 16 while Faulkner (**18**) finds similar values for stars associated with the more highly excited parts of the H II region. The colour excess of 0·69 may be further compared with the value 0·60 derived by Faulkner & Aller (**19**) for their region 'a' of the H II region some 3′ to the north of η Carinae; these values are highly consistent when one considers that η Carinae appears to lie in a fainter (possibly more highly obscured) region of the nebula.

Johnson (**20**) has recently presented observations reopening the question of the ratio of total visual absorption to colour excess. His data suggest that the value $R=A_v/E_{B-V}=3{\cdot}0$ may be a minimum value in the galactic plane and that in some regions, ratios as high as $R=6{\cdot}6$ may be appropriate. Since, as mentioned above, there is considerable evidence that the OB stars in Carina are extensive in depth, it is extremely difficult to determine directly this ratio through the method of 'differential reddening' of objects which are assumed to be at a common distance. However, if we adopt Faulkner's criterion that stars inside the high excitation contour of the H II region are more likely to be involved in it then a plot of their apparent moduli against colour excess implies a value of R between 6 and 10. The data given by Faulkner are inconsistent with R as low as 3·0 unless we accept that only one O5 star is responsible for the excitation of the H II region and that it is isolated in space from the other early type stars in the region.

Mr Maston Beard and Dr F. J. Kerr have kindly provided data on the radio brightness at 11 cm from a circular area, diameter 7·5′, of the H II region centred

on η Carinae. A comparison of the radio emission measure with the photoelectric measurements we have made of the brightness of the same region in Hα light gives a direct measure of $A_{H\alpha}$. The derived value of R is 5·3 with an estimated uncertainty of 15%. We consequently adopt $R=6{\cdot}0$ in our discussion of η Carinae. In this case the absolute flux from the continuum of η Carinae at 5560 Å is $4{\cdot}84\times10^{-10}$ erg/cm²s Å. We have plotted in Fig. 2, along with the observed data, the continuum corrected for the derived value of the colour excess. Absorption was taken to be inversely proportional to wavelength over the observed wavelength range.

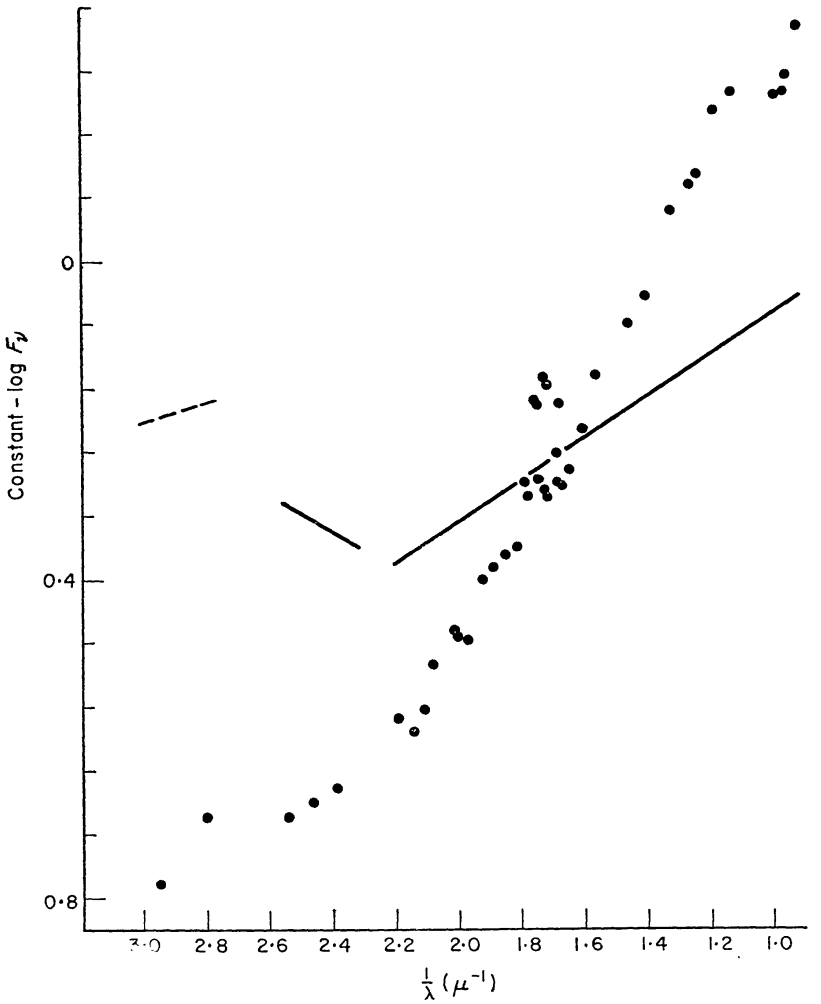

FIG. 2. *The continuum energy distribution of η Carinae. The observed (dots) and corrected (line) continua are shown in the form, constant $-\log F_\nu$ plotted against frequency $1/\lambda/(\mu^{-1})$.*

(*c*) *Emission line intensities.* We have measured the intensities of lines of the Balmer and Paschen series, of [N II], [S II], [Ne III] and He I. With the exception of the Paschen lines, the equivalent widths were measured in terms of the continuum seen on microphotometer intensity tracings of the high-dispersion spectra obtained in the 1964 observing season. The equivalent widths of Pγ, Pδ and Pε were measured directly from the scanner tracings. The scanner observations were then used to relate the equivalent widths to the line

intensity ratios. The equivalent widths for the Paschen lines might be suspected of being affected by blending due to the low resolution of the scanner material; however, reference to Fig. 1 will show these lines to dominate the emission at the appropriate wavelengths. In Table III we present the absolute fluxes for the lines measured together with absolute strengths of the underlying continuum.

TABLE III

*Emission line intensities in η Carinae**

Line	Continuum flux (erg/cm² s Å)	Line flux (erg/cm² s)
Pγ	$2{\cdot}18 \times 10^{-10}$	$3{\cdot}56 \times 10^{-8}$
Pδ	$2{\cdot}40 \times 10^{-10}$	$2{\cdot}42 \times 10^{-8}$
Pε	$2{\cdot}61 \times 10^{-10}$	$1{\cdot}49 \times 10^{-8}$
Hα	$4{\cdot}14 \times 10^{-10}$	$3{\cdot}74 \times 10^{-7}$
Hβ	$5{\cdot}48 \times 10^{-10}$	$6{\cdot}25 \times 10^{-8}$
Hγ	$6{\cdot}14 \times 10^{-10}$	$2{\cdot}69 \times 10^{-8}$
Hδ	$7{\cdot}32 \times 10^{-10}$	$1{\cdot}39 \times 10^{-8}$
[S II] 6730	$4{\cdot}01 \times 10^{-10}$	$5{\cdot}59 \times 10^{-10}$
[S II] 6716	$4{\cdot}05 \times 10^{-10}$	$1{\cdot}26 \times 10^{-10}$
[S II] 4076	$7{\cdot}50 \times 10^{-10}$	$8{\cdot}55 \times 10^{-10}$
[S II] 4068	$7{\cdot}54 \times 10^{-10}$	$4{\cdot}37 \times 10^{-9}$
[N II] 6584	$4{\cdot}14 \times 10^{-10}$	$3{\cdot}52 \times 10^{-9}$
[N II] 6548	$4{\cdot}19 \times 10^{-10}$	$8{\cdot}38 \times 10^{-10}$
[N II] 5755	$4{\cdot}69 \times 10^{-10}$	$8{\cdot}92 \times 10^{-9}$
[Ne III] 3868	$9{\cdot}60 \times 10^{-10}$	$1{\cdot}69 \times 10^{-9}$
He I 10830	$2{\cdot}22 \times 10^{-10}$	$5{\cdot}79 \times 10^{-8}$
He I 5875	$4{\cdot}60 \times 10^{-10}$	$8{\cdot}29 \times 10^{-9}$
He I 4471	$5{\cdot}84 \times 10^{-10}$	$2{\cdot}62 \times 10^{-9}$
[O III] 5015	$5{\cdot}32 \times 10^{-10}$	$< 1{\cdot}33 \times 10^{-10}$
[O III] 4959	$5{\cdot}41 \times 10^{-10}$	$< 1{\cdot}35 \times 10^{-10}$
[O III] 4363	$6{\cdot}11 \times 10^{-10}$	$< 1{\cdot}53 \times 10^{-10}$
[O II] 3727	$1{\cdot}17 \times 10^{-9}$	$< 2{\cdot}92 \times 10^{-10}$
[O II] 3729	$1{\cdot}15 \times 10^{-9}$	$< 2{\cdot}89 \times 10^{-10}$

*N.B. Reddening corrections have been applied

(*d*) *Photometric errors.* The errors that exist in the data given in Tables I–III are not formally derivable. In this section we shall give estimates of the errors that may affect the measurements of the lines and continua. An intercomparison of the results of the scanner photometry on each of the five nights η Carinae was observed with a blue sensitive cell indicates probable errors of about $0^m{\cdot}07$ at all wavelengths shorter than λ 5500 Å. The scanner response at λ 5840 Å is one hundredth that of the response at λ 4100 Å and one fiftieth of that at λ 3300 Å. Blue cell scans above λ 5500 Å have a mean error as large as $0^m{\cdot}12$. The results however are strengthened by the infra-red scans which overlap in this region. Up to λ 6800 Å the infra-red scans have similar probable errors of $0^m{\cdot}07$; longward of λ 6800 Å errors in the continuum depend in part on the interpretation of the red scans. The probable error of the reduced continuum data from the five

nights on which infra-red scans were made is $\pm 0^{m}\cdot06$ illustrating that the adopted continua had considerable consistency in spite of the variations in time constant, resolution and amplifier sensitivity affecting different sections of each scan. Within these errors there was no secular variation in the continuum over the period of observation. The errors involved in deriving the absolute flux of the continuum of η Carinae at λ 5560 Å are dominated by the uncertainties of the observations of η Carinae rather than of the Oke standards. The absolute flux was determined from both blue and infra-red cell observations and has a probable error of $\pm 0^{m}\cdot09$. Our determination of the interstellar reddening of η Carinae is, of course, an indirect one. It could be vitiated by large changes in the absorption over distances of 20″ or by internal absorption in η Carinae itself. Both these conditions appear implausible to us. The probable error of the determination of the colour excess of the H II region observed is $0^{m}\cdot06$.

Our experience of spectrophotometry with the coudé spectrograph at Mount Stromlo suggests that with absorption line photometry, errors larger than 10% are unlikely. In the case of η Carinae enormous variations in the intensities of the emission lines relative to the reference continuum are encountered. We found that for the weaker lines (equivalent widths up to 40 Å) the photoelectric and photographic data differed by less than 6%. For the stronger lines and in particular for Hα, there appeared consistent discrepancies in that the photographic data gave larger equivalent widths. Remembering that for Hα (E.W. = 904 Å) the peak line intensity is several hundred times that of the continuum, it will be appreciated why we placed more reliance on the linearity of response of the photomultipler and adopted the equivalent width as measured on the scanner tracings.

There is little published quantitative data available with which to compare our measures. Thackeray (3) has estimated the relative strengths of the emission lines in η Carinae. We compare in Fig. 3 the line strengths given by Thackeray with the measured intensities of Table III.

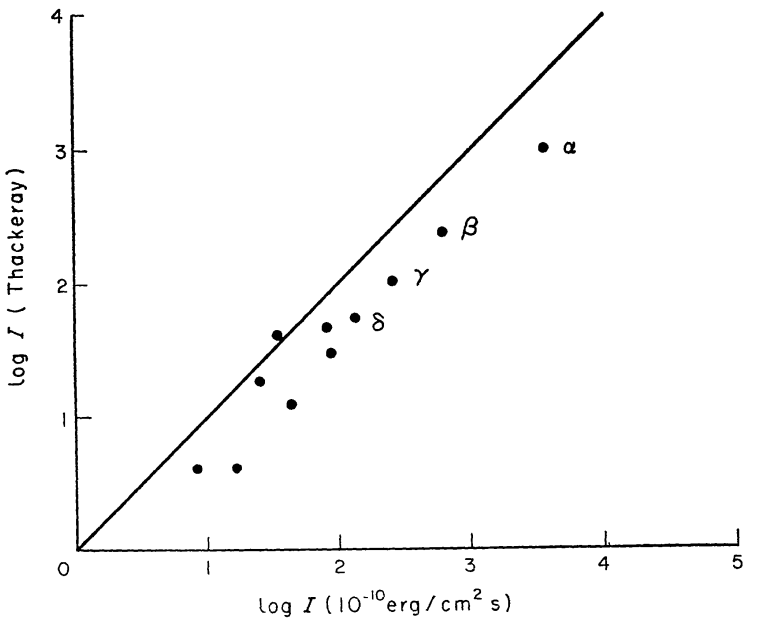

FIG. 3. *Calibration of the intensities of the emission lines in η Carinae estimated by Thackeray. Points representing the Balmer lines are marked α, β, γ and δ.*

There is excellent consistency between these two sets of data; in comparison with the absolute unreddened line intensities there is remarkable linearity in Thackeray's intensity scale over a wide range of line strengths.

4. *Discussion*

(*a*) *Distance and size of η Carinae.* As mentioned above half the light of η Carinae is emitted from a region within 2·5″ of the nucleus and we shall take this to define an effective radius of η Carinae. Thackeray (**15**) places η Carinae at a distance of 1·2–1·9 kpc. The estimates are based on the nova-parallax and the assumed relation of η Carinae to the surrounding cluster Trumpler 16. Feinstein's photometry (**12**) of this cluster (assuming $A_v = 3{\cdot}0\,E_{B-V}$) leads to a distance of 2800 pc. Faulkner (**18**) obtains a distance of 2500 pc for the stars in the high excitation part of the H II region; he also took A_v to be $3{\cdot}0\,E_{B-V}$. If A_v/E_{B-V} in the region of η Carinae is as high as 6·0, Faulkner's distance for these stars becomes 1250 pc. In addition, Gratton (**16**) has discussed the problem of the distance of η Carinae and concludes that a distance of 1·5 pc is consistent with the available observations. We shall follow Gratton and adopt 1500 pc as the distance of η Carinae. At the adopted distance of 1500 pc, the effective radius is $5{\cdot}5 \times 10^{16}$ cm.

(*b*) *The forbidden line spectrum.* Among the emission lines in the spectrum of η Carinae which have been identified by Thackeray (**3**, **4**), there are many arising from forbidden transitions in the ions of singly ionized nitrogen, sulphur, iron and nickel. Thackeray has shown that within the errors of measurement (2 km/s) these lines have the same radial velocity. In addition our own observations show that these lines have similar profiles.

The hydrogen recombination lines also show major components with velocities identical to the forbidden lines. We conclude that the forbidden lines of N II, S II, Fe II and Ni II originate in the same regions of η Carinae. The presence of N II implies that in these regions hydrogen is predominantly ionized. If hydrogen were *radiatively* ionized there would be no appreciable number of singly ionized iron atoms.

We find that the total energy radiated in the lines of Fe II is approximately equal to the energy radiated in the lines of the Balmer series. This implies that the ratio of Fe^+ ions to protons must be roughly equal to the ratio of the proton–electron recombination cross section to the collisional excitation cross sections for Fe^+. A reasonable estimate for this ratio is 10^{-5}. In the regions of η Carinae where the hydrogen is ionized most of the iron is singly ionized. Our conclusion is that the co-existence of ionized hydrogen and singly ionized nitrogen and iron proves that the ionization in η Carinae is by collisional processes.

House (**21**) has made non-thermodynamic equilibrium calculations of the relative concentrations of ions for various elements over a wide range of electron temperatures. Collisional ionization and radiative and collisional recombination were taken to be the processes controlling the ionization equilibria. On the basis of House's computations the electron temperature of a gas in which there are significant concentrations of N II, S II and Fe II, lies between 18 500 and 23 000 °K.

Another group of emission lines in η Carinae arises from forbidden transitions in the spectra of Ne III, Ar III, Fe III and the recombination spectrum of He I.

These lines undergo simultaneous variations in intensity. We have obtained high dispersion spectra of η Carinae in 1964 March, 1965 February and 1966 February. The lines are present in similar strength relative to the continuum on the 1964 and 1966 plates while in 1965 the lines are undetectable. Gaviola observed a similar fading in 1949. The fact that the lines vary relative to the lines of lower ionization suggests that they originate in a different region from that characterized by an electron temperature of around 20 000 °K, and the fact that they vary *together* suggests that they originate in regions with electron temperatures and densities in common. The co-existence of ions of He II, Ne III, Ar III and Fe III in appreciable abundance implies an electron temperature between 41 000 and 54 000 °K.

Under conditions of collisional ionization, it is impossible to understand the co-existence of singly ionized sulphur and doubly ionized neon at any electron temperature so that, in addition to the evidence given by the variability of the high excitation lines, there is a strong indication of inhomogeneities in η Carinae. We note that the above derivation of electron temperatures makes no specific assumption concerning relative abundances in η Carinae.

We turn now to a computation of the specific emissivities (erg/s atom) of some of the forbidden lines in the spectrum of η Carinae.

The common ground configuration of ions from which forbidden transitions of interest arise consists of three terms well separated from the first excited state, each of which may be multiple. In what follows we shall label these levels, 1, 2 and 3 in order of increasing excitation.

The intensity I_{nm} of the forbidden line may be written

$$I_{nm} = N_n A_{nm} h\nu_{nm} \tag{1}$$

where N_n is the population of the excited state, A_{nm} the transition probability and ν_{nm} the frequency. Under conditions of collisional ionization we can express N_n in terms of the abundance of the atomic species through the use of Parker's (**22**) normalization of Elwert's ionization formula,

$$N(X^+)/N(X) = C(\zeta_n/n)(\chi_H/\chi_n)^2(kT/\chi_n)\exp(-\chi_n/kT) \tag{2}$$

where $C = 2{\cdot}7 \times 10^5$, $N(X^+)/N(X)$ is the relative number of atoms in successive stages of ionization, ζ_n is the number of electrons in the outermost shell, n, of the parent atom or ion, χ_H/χ_n is the ratio of the ionization potential of hydrogen to that of the parent atom or ion and T_e is the electron temperature, together with the formulae giving the relative population N_n of the excited levels, 2 or 3, in terms of the ionic abundance N. We assume that each ion is only populated in levels 1, 2 or 3.

Assuming a Maxwellian velocity distribution of the free electrons and neglecting radiative excitation and induced emissions, the relative population of levels 1, 2 and 3 are given by

$$N_2/N_1 = (q_{12} + q_{13}(A_{32} + q_{32})/(A_{31} + A_{32} + q_{31} + q_{32}))/(A_{21} + q_{21} + (q_{23}(A_{31} + q_{31}))/(A_{21} + A_{32} + q_{31} + q_{32}) \tag{3}$$

and,

$$N_3/N_2 = ((q_{13}(q_{23} + q_{21} + A_{21})) + q_{23}q_{12})/(q_{12}(A_{31} + A_{32} + q_{31} + q_{32}) + q_{13}(q_{32} + A_{32})). \tag{4}$$

Then,

$$N_2/N=(N_2/N_1)/(1+N_2/N_1+(N_3/N_2)(N_2/N_1)) \quad (5)$$

and,

$$N_3/N=(N_3/N_2).(N_2/N_1)/(1+N_2/N_1+(N_3/N_2)(N_2/N_1)). \quad (6)$$

In equations (3) and (4) q_{mn} and q_{nm} are the rates of collisional excitation and de-excitation respectively and A_{mn} is the Einstein spontaneous emission coefficient. The rate of de-excitation is given by

$$q_{mn}=8{\cdot}63\times10^{-6}(\Omega_{mn}/\omega_n).(N_e/T_e^{1/2}) \quad (7)$$

where N_e and T_e are the electron density and temperature, Ω_{mn} the target area parameters for the transition, and ω_n the statistical weight of the upper level. The excitation rate is related to q_{nm} by,

$$q_{mn}=q_{nm}(\omega_n/\omega_m)\exp(-E_{nm}/kT_e) \quad (8)$$

where E_{nm} is the difference in energy between levels n and m.

Using the IBM 1620 computer at Mount Stromlo we have calculated I_{nm} according to equations (1–8) for the forbidden transitions listed in Table III in the range of electron temperature 5×10^3 to 10^5 °K, and density from 4×10^2 to 4×10^9/cm^3. The transition probabilities and target area parameters listed by Seaton (**23**, **24**) were used in the computations. Similar calculations have been made by Parker (**22**) who restricted himself to an electron density of 400/cm^3.

(*c*) *Conditions in the cooler ionized region.* Using the results of the calculations described above we can demonstrate the dependence of the internal forbidden line ratio, (I_{32}/I_{21}) for N II, (i.e. $I_{5755}/I_{6548+6584}$) on electron density at temperatures near 20 000 °K. We plot, in Fig. 4, the computed logarithm of the line intensity ratio against electron density. The value of the observed ratio, also shown in Fig. 4, is taken from the data in Table III and indicates an electron

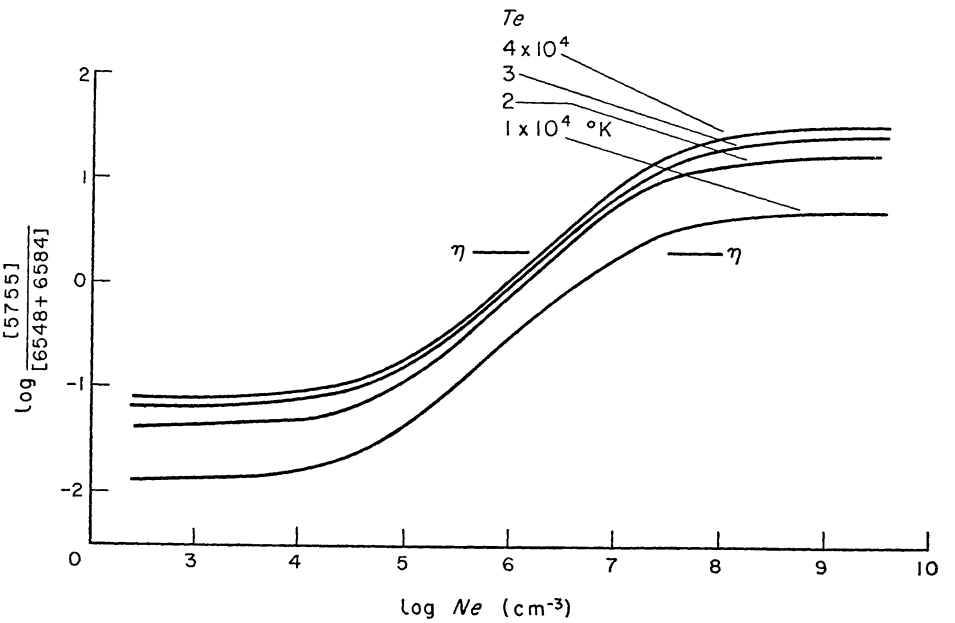

FIG. 4. *The dependence of the line intensity ratio, $I_{5755}/I_{6548+6584}$ for N II on electron temperature and density.*

density of $3 \times 10^6/cm^3$ for the cooler ionized region of η Carinae. Similarly the line ratio I_{31}/I_{21} for [S II] indicates an electron density of $3 \times 10^5/cm^3$. We place greater weight on the value derived from the [N II] lines because of the more precisely known collisional parameters. In both the case of the [N II] and [S II] lines, the internal line ratios are relatively insensitive to electron temperature. However, some dependence on electron temperature exists in the line ratios of, for example $[N\,II]_{21}/[S\,II]_{21}$. Before comparing the intensities of lines of different elements, some assumptions must be made regarding the relative atomic abundances in η Carinae. In Fig. 5 we show the locus of the observed line ratios, $[N\,II]_{32}/[N\,II]_{21}$ and $[N\,II]_{21}/[S\,II]_{21}$ in terms of the parameters, T_e and N_e for an assumed nitrogen, sulphur abundance ratio of 3·0. The effect on the derived temperature of adopting N/S ratios of 1·0 and 10·0 are also shown in Fig. 5. The expected consistency of the electron temperatures found in Fig. 5 with the temperatures derived from the discussion of ionization levels is apparent.

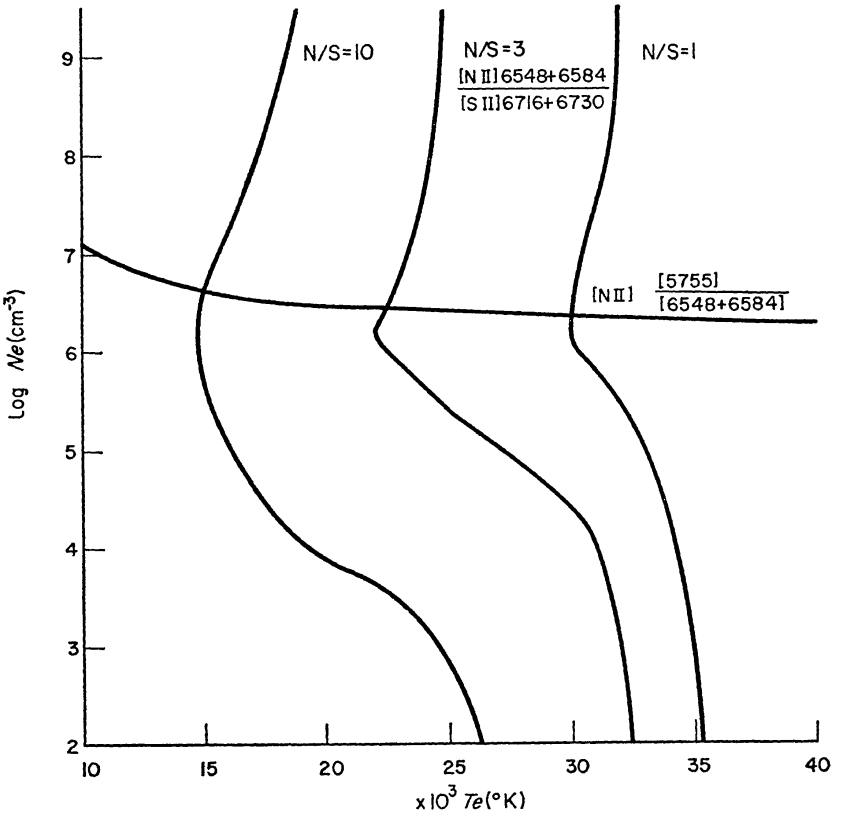

FIG. 5. *The T_e, log N_e relations for η Carinae defined by the observed line ratios* $[N\,II]_{6548+6584}/[S\,II]_{6716+6730}$ *and* $[N\,II]_{5755}/[N\,II]_{6548+6584}$ *for assumed N/S abundance ratios of* 10, 3 *and* 1.

We adopt an electron temperature of 22 000 °K and an electron density of $3 \times 10^6/cm^3$ for the cooler ionized region in η Carinae.

A major feature of the spectrum of η Carinae is the absence of the forbidden lines of [O II] λ3727 + 3729 Å and [O III] λ5015 + 4959 Å. At temperatures around 20 000 °K most of the oxygen present should be in the form of O II. We enquire then whether the observed absence of [O II] λ3727 + 3729 Å can be reconciled with the temperature and densities we have found for the cooler

ionized region of η Carinae or whether the absence of these lines is indeed due to an abundance deficiency of oxygen as suggested by Thackeray.

Let us assume for the purposes of our initial discussion that atomic abundances in η Carinae follow those in the B stars of the galactic plane and, from Aller (**25**) take these to be H: 10^5; O and Ne, 75; N, 15 and S, 5 by atom. We also assume that the [O II] emission occupies the same volume as does the [N II] emission. We now compare the intensities of the [N II] λ5755 Å line and the [N II] λ6548+6584 Å lines with that of [O II] λ3727+3729 Å. The observed line ratios are [N II] λ5755 Å/[O II] λ3727+3729 Å $\geqq 15$ and [N II] λ6548+6584 Å/[O II] λ3727+3729 Å $\geqq 7{\cdot}5$. At an electron temperature of 22 000 °K and an electron density of 3×10^6/cm^3 the ratios of the emissivities (erg/s atom) of [N II] λ5755 Å and [N II] λ6548+6584 Å to that of [O II] λ3726+3729 Å are 40 and 18 respectively. The ratios of the volume emissivities (erg/cm^3 s) are then 8 and 3·6. A comparison of the ratios of the volume emissivities with the observed line intensity ratios leads to the conclusion that the [O II] lines are weaker than predicted by at least a factor 2. We further find that no variation of the electron temperature or density over plausible limits (3×10^5–10^7/cm^3 in density and 10 000–30 000 °K in temperature) will allow us to reconcile the observed absence of [O II] lines with the O/N ratio given above.

An evaluation of the significance of these results hinges on the accuracy of the numbers which we have taken to represent 'normal abundances' of young stars in the galactic plane. There is in the data listed by Aller (**25**), a scatter from star to star in the O/N ratio of a factor of about 2. Whether this scatter is intrinsic or due solely to errors in the analyses we conclude that it is just possible that the absence of the [O II] lines may be reconciled with the observed range of abundances in galactic B stars.

In order to determine the volume from which the forbidden line emission arises, we must compare the measured absolute fluxes (erg/s) with the computed emissivities (erg/s atom) and, since the ionization of hydrogen is nearly complete at temperatures of 20 000 °K, assume a value for the abundance ratio of hydrogen to the appropriate element. We will again adopt the abundance values from Aller (**25**) and discuss the lines [N II] λ5755 Å and [N II] λ5648+6584 Å. There are then 450 N atoms/cm^3 in the cooler ionized region of η Carinae. A comparison of the observed fluxes and computed emissivities leads to $5{\cdot}1 \times 10^{50}$ as the number of N atoms involved occupying a volume of $1{\cdot}1 \times 10^{48}$ cm^3. Similarly from the absolute brightness of the [S II] lines we find an emitting volume of $1{\cdot}2 \times 10^{48}$ cm^3. The agreement in the derived volumes of emission from sulphur and nitrogen shows that the N/S abundance ratio in η Carinae is close to that adopted. The volume of a sphere of radius $5{\cdot}5 \times 10^{16}$ cm is $5{\cdot}2 \times 10^{50}$ cm^3.

(*d*) *Conditions in the hotter ionized region.* We have shown that the presence of ephemeral emission lines of [Ne III], [Ar III], [Fe III] and the recombination lines of He I implies the existence at times, of a hotter ionized region in η Carinae in which the electron temperature is typically 50 000 °K.

At this temperature the majority of the oxygen in the regions is doubly ionized, however the lines [O III] λ4959+5015 Å and [O III] λ4363 Å are unobservable on our spectrograms of η Carinae. We assume that the [Ne III] and [O III] emission are coextensive, and attempt to find conditions which will reproduce the observed line intensity ratios, [Ne III] λ3868 Å/[O III] λ4959+5015 Å $\geqq 6{\cdot}3$

and [Ne III] λ3868 Å/[O III] λ4363 ≧ 11, with an assumed Ne/O abundance ratio of unity. With these assumptions the computed relative line intensities are equal to the ratios of the specific emissivities. In Table IV we show the ratios of the emissivities for [Ne III] λ3868 Å/[O III] λ4959 + 5015 Å at various electron temperatures and densities.

TABLE IV

Relative emissivities, [Ne III] λ3868 Å/[O III] λ4959 + 5015 Å

N_e (cm^{-3}) / T_e (10^4 °K)	4×10^2	4×10^6	4×10^9
3	$3{\cdot}4 \times 10^{-3}$	$1{\cdot}3 \times 10^{-1}$	$7{\cdot}3 \times 10^{-1}$
4	$9{\cdot}1 \times 10^{-2}$	$3{\cdot}1 \times 10^{-1}$	1·7
5	$2{\cdot}6 \times 10^{-1}$	$8{\cdot}5 \times 10^{-1}$	5·5
6	$4{\cdot}4 \times 10^{-1}$	1·4	9·8
7	$5{\cdot}9 \times 10^{-1}$	1·8	14
8	$8{\cdot}5 \times 10^{-1}$	2·5	19
9	1·1	3·1	25
10	1·3	3·8	30

In Table IV we can see that to meet the observed ratio of ≧ 6·3 at electron temperatures near 50 000 °K we require densities greater than 10^9/cm^3.

The consideration that the recombination time must be less than a year to explain the variation of the high excitation lines is certainly consistent with this density; it leads to a lower limit of N_e of 2×10^5/cm^3.

However, while we have been able to find conditions in both the hotter and cooler ionized regions in η Carinae in which the absence of lines of [O III] and [O II] could be reconciled with the presence of lines of other elements in their observed strengths, our continuing spectrophotometry of outlying regions of η Carinae reveals no trace of forbidden oxygen lines anywhere. Our discussion of the results of spectrophotometry in these regions will be given in a later paper; however it seems already evident that conditions quite different from those in the central parts pertain there. On these grounds we conclude that oxygen is indeed deficient relative to sulphur and nitrogen in η Carinae.

We compute the effective volume of the hotter ionized regions of η Carinae assuming (a) $N_e = 4 \times 10^6$/cm^3 and (b) $N_e = 4 \times 10^9$/cm^3. The emissivity of the lines [Ne III] λ3868 + 3969 Å at $T_e = 50\,000$ °K and $N_e = 4 \times 10^6$/cm^3 is $1{\cdot}45 \times 10^{-14}$ erg/s atom and at $T_e = 50\,000$ °K and $N_e = 4 \times 10^9$/cm^3 is $1{\cdot}31 \times 10^{-13}$ erg/s atom, so that with the previously adopted H/Ne ratio we find that the radiation arises in a volume of $1{\cdot}28 \times 10^{46}$ cm^3 for case (a) and $1{\cdot}42 \times 10^{42}$ cm^3 for case (b).

(*e*) *The Balmer line radiation.* The Balmer line profiles show evidence of self-absorption which is shared by the strong permitted emission lines of other elements but not by the strong forbidden lines. In the permitted emission lines this is seen as a blue displaced (by about 60 km/s) absorption nick in the emission profiles. At about 500 km/s to the blue of each of the Balmer lines a strong, wide absorption component is seen. This component, of nearly the same width as the emission lines, not only absorbs light from the continuum

but also strongly affects the emission profiles. In Table V we list the half-widths of the emission components of Hβ, Hγ and Hδ.

TABLE V

Half-widths of Balmer emission lines

	Hβ	Hγ	Hδ
W(Å)	9·6	6·5	5·3
$W/\lambda \times 10^4$	1·98	1·50	1·29

The inequality $W_\beta/\lambda_\beta > W_\gamma/\lambda_\gamma > W_\delta/\lambda_\delta$ shows that the absorption component steepens the observed Balmer emission decrement and that the absorption decrement is flatter than the emission decrement.

We have plotted, in Fig. 6, the observed Balmer decrement in the form log $I(H\beta/H\gamma)$ against log $I(H\alpha/H\beta)$. For comparison we show points representing the decrement computed by Capriotti (**26**) for a radiatively ionized gas under the conditions of case B with various optical thicknesses in Hα. We also plot the Balmer decrement computed by Parker (**22**) for collisional excitation of the hydrogen by electrons at 10^4, 2×10^4 and 4×10^4 °K, again under case B conditions. It can be seen that the observed decrement in η Carinae does not fit any of the above cases. A match to the computed radiative decrements could be obtained if the reddening we have derived is approximately half the true value but for reasons given earlier we do not believe that this can be the case. We conclude that η Carinae is not radiatively excited.

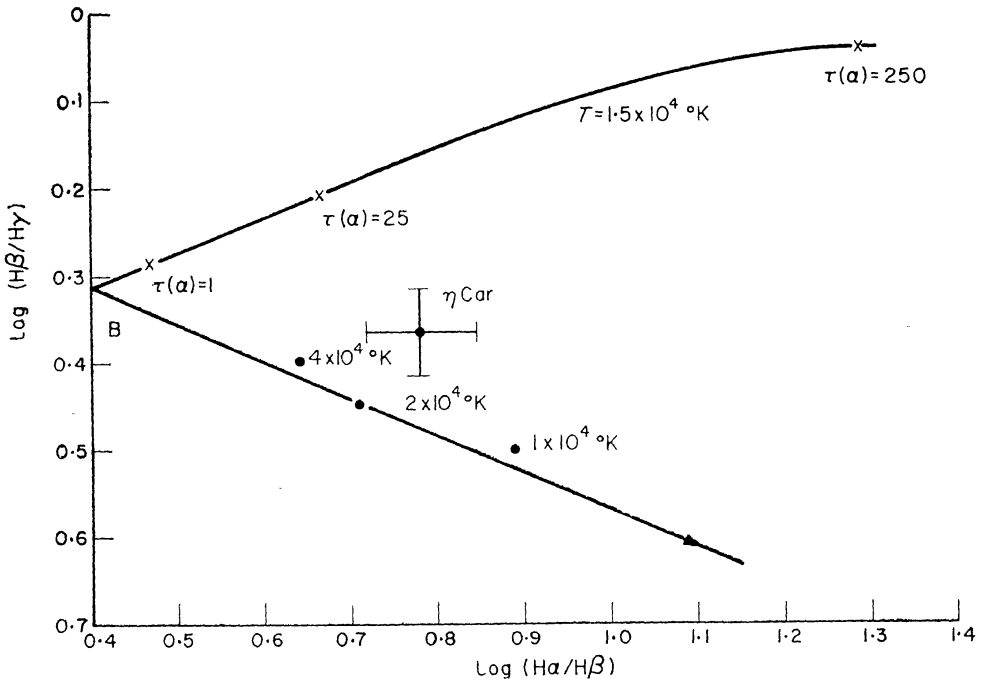

FIG. 6. *The comparison of the observed and computed Balmer decrements. The radiative decrements for various optical depths in Hα are shown by crosses, the collisional decrements by dots. The point B (log Hβ/Hγ=0·32, log Hα/Hβ=0·4) represents the recombination decrement for case B and an electron temperature of 10^4 °K computed by Burgess. The arrowed line represents the effect of interstellar reddening. The error bars represent the estimated uncertainty in the decrement in η Carinae.*

The observable portion of the Paschen decrement does not add much information on the mode of ionization.

In Table VI we show the computed Paschen decrements for electron temperatures of 10^4, 2×10^4 and 4×10^4 °K, together with the observed decrement.

TABLE VI

	Radiative			Collisional			Observed
T(°K)	10^4	2×10^4	4×10^4	10^4	2×10^4	4×10^4	
log $P\gamma/P\delta$	0·218	0·208	0·208	0·277	0·243	0·225	0·168 ± 0·06
log $P\delta/P\epsilon$	0·165	0·165	0·166	0·203	0·185	0·178	0·210 ± 0·06

The observed decrement fits no case well and on the other hand the observational errors are such that it provides no discriminant between them.

The observed flux in the Balmer lines and continuum of η Carinae in principle enables us to determine the product $N_e^2 \times$ the volume of the object. The line radiations are so strongly self-absorbed that the usual theories applicable to optically thin nebulae are hardly relevant in this case. However, two estimates of $N_e^2 \times V$ can be made, one from the Hα flux and the other from the flux in the Balmer continuum. The resulting values of $N_e^2 V$ are not in good agreement.

The upper levels of the Balmer transitions are populated by recombination and by collisional excitation. For a nebula which is optically thick in the Balmer lines, each process which populates the levels $n \geqq 3$ results in the emission of an Hα photon. We assume this to be true in η Carinae.

The emission coefficient per unit volume for Hα is given by

$$j_{32} = Ne^2(\alpha_{32} + \gamma_{32})h\nu_{32} \tag{9}$$

where α_{32} is the effective recombination coefficient. Using the calculations of Burgess (**17**) we find that with $T_e = 2 \times 10^4$ °K, $\alpha_{32} = 7{\cdot}7 \times 10^{-14}$ cm³/s. γ_{32} accounts for the collisional excitation. An estimate is given by

$$N_e \,.\, N_i \,.\, \gamma_{32} = q \sum_{n=3}^{\infty} N_e \,.\, N_1(\mathrm{H}) \,.\, \alpha(1\mathrm{s} - \mathrm{np}) \tag{10}$$

where N_e is the electron and N_i the proton density, N_1(H) is the density of neutral hydrogen, q is the ratio of the number of collisional excitations to all states to the number of collisional excitations to p states, and the $\alpha(1\mathrm{s} - \mathrm{np})$ are collision excitation cross sections. Parker (**22**) lists values of $\alpha(1\mathrm{s} - \mathrm{np})$. For q we take as an approximation that

$$q = 1 + 1{\cdot}5\{\alpha(1\mathrm{s} - 2\mathrm{s})/\alpha(1\mathrm{s} - 2\mathrm{p})\}. \tag{11}$$

For $T_e = 2 \,.\, 10^4$ °K, we find $\gamma_{32} = 3{\cdot}5 \times 10^{-13}$ cm³/s. The total luminosity of η Carinae in the Hα line is $9{\cdot}55 \times 10^{37}$ erg/s. We derive the result that

$$N_e^2 V = 1{\cdot}0 \times 10^{62}\ \mathrm{cm}^{-3}.$$

The continuum flux at λ3600 Å outside the Earth's atmosphere and corrected for interstellar absorption is $1{\cdot}34 \times 10^{-9}$ erg/cm² s Å. Of this 44% is accounted for by the extrapolated red continuum of η Carinae which we have assumed to have the form $F_\nu \propto e^{-\alpha\nu}$. The remainder we suppose to result from hydroger recombination. Using the recombination coefficients tabulated by Seator at the adopted temperature of $T = 20\,000$ °K, we derive a value of $N_e^2 V$ o $7{\cdot}8 \times 10^{62}$ cm⁻³.

We can conclude from these considerations only that $N_e^2 V$ is of the order of $10^{62}/\text{cm}^{-3}$. The value of N_e derived from the forbidden lines is $3 \times 10^6/\text{cm}^3$ so the volume of hydrogen emission is 10^{49} cm^3. This volume is to be compared with the adopted volume of η Carinae of 5×10^{50} cm^3 and with the volume derived from the forbidden line emission on the assumption of a normal hydrogen ratio which was 10^{48} cm^3. These comparisons suggest two things; first that the assumed uniformity of the electron density is an over-idealization and that appreciable density fluctuations exist in η Carinae, and secondly that nitrogen and sulphur are under-abundant with respect to hydrogen (as compared with main sequence B stars) as we have already concluded oxygen to be.

(*f*) *Mass and energy balance.* A minimum mass for η Carinae follows from the preceding discussions. The total mass certainly exceeds that of a volume of 10^{49} cm^3 filled with ionized hydrogen with an electron density of $3 \times 10^6/\text{cm}^3$ or 5×10^{31} g ($0{\cdot}025\ M_\odot$). An upper limit on the mass can be estimated by assuming that the entire volume of 5×10^{50} cm^3 is filled by (mainly neutral) hydrogen at the same density. This upper limit is about $1\ M_\odot$.

With the distance modulus adopted in this paper, the visual absolute magnitude of η Carinae at light maximum was near -16 and the total outburst has involved a radiation of near 2×10^{50} erg, an amount of energy that could be supplied by the conversion of $0{\cdot}2\ M_\odot$ of hydrogen into helium. At the present time in the continuum between 3000 Å and 10000 Å η Carinae radiates 8×10^{38} erg/s. The energy radiated in the Balmer lines is about 1×10^{38} erg/s and the energy radiated in other lines (mostly Fe II) is about the same.

If the cooling of the gas in η Carinae occurs through the observed line radiation then to maintain equilibrium an energy supply of 2×10^{38} erg/s is required. The only obvious source of such energy is the kinetic energy of the observed mass of η Carinae. The observed minimum mass of η Carinae is 5×10^{31} g and typical velocities of 500 km/s give an available energy source of 6×10^{46} erg which would supply sufficient energy over a period of 10 years. The kinetic energy could maintain the observed mass of ionized hydrogen over the relevant time scale of about a century if the mass of neutral hydrogen were 10 times larger than the ionized material. In these circumstances the outburst in η Carinae would have involved a mass of $0{\cdot}2\ M_\odot$ and a kinetic energy of 10^{49} erg.

5. *The continuum*

(*a*) *The problem.* The bulk of the energy radiated by η Carinae is in the continuum and indeed the principal result of this investigation has been to bring to attention the existence of a featureless continuum of the form shown in Fig. 2.

The continuum appears to have two components. Below λ3650 Å there is obviously a contribution from a Balmer recombination continuum. Longward of λ4600 Å there is a second component which dominates the Paschen and Bracket recombination continua and which can be expressed as $F_\nu \propto e^{-\alpha\nu}$ where $\alpha = 2{\cdot}54 \times 10^{-15}$ c.g.s. units. In order to show clearly the way in which the observed continuum differs from that due to the thermal emission of ionized hydrogen we compare in Fig. 7 the observed continuum with a hydrogen recombination and free–free continuum which, following Seaton (**27**), we have computed for

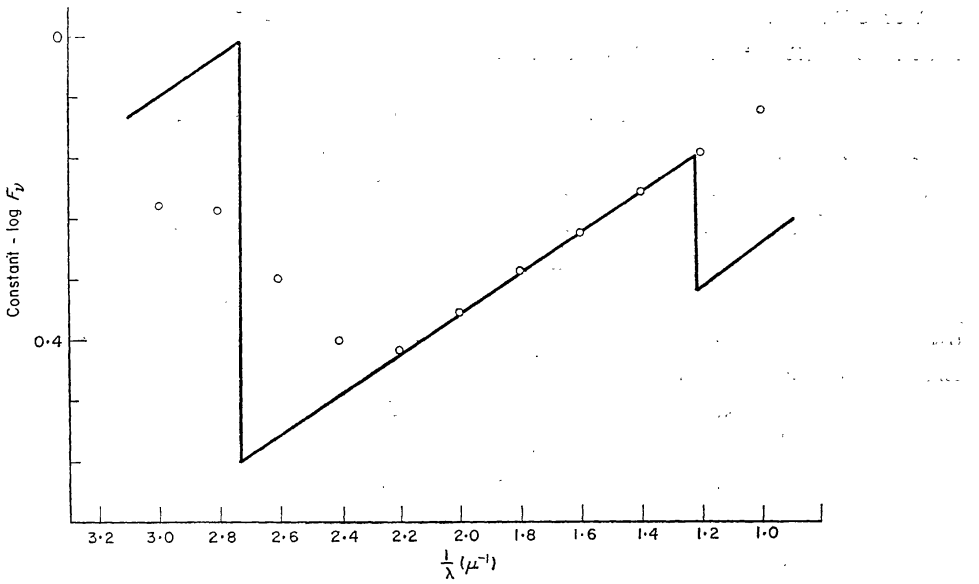

FIG. 7. *The continuum energy distribution in η Carinae (circles) compared with a computed hydrogen recombination and free–free continuum for an electron temperature of 24 000 °K. Levels up to n = 10 have been included in the computation and two photon emission neglected.*

an electron temperature of 24 000 °K. Two photon emission has been neglected as the electron density exceeds 10^5/cm^3. At the assumed electron temperature of 24 000 °K the slope of the observed continuum longward of λ4600 Å matches the computations. However the observed and computed discontinuities are entirely discordant and the absence of a Paschen discontinuity finds no explanation. The absence of a Paschen discontinuity (which certainly cannot exceed $0^m{\cdot}09$) and the presence of a Balmer discontinuity of $0^m{\cdot}80$ cannot be reconciled with a hydrogen recombination spectrum at any assumed electron temperature.

The problem is then to understand the nature of the red continuum in η Carinae.

(*b*) *The stellar hypothesis.* We have considered the possibility that the continuum might be stellar although, as we have previously remarked, the nucleus of η Carinae is non-stellar in appearance. Stars of spectral type near Go best fit the slope of the red continuum, but in a log F_ν–ν plot show a pronounced curvature quite unlike the η Carinae continuum. In the spectrum of η Carinae there are several windows free of emission lines and in these regions the continuum is smooth and featureless. Examples of such regions are λλ 5673–5724, 4966–4922, 4672–4695 and 4590–4060 Å. If the redward component of the continuum of η Carinae is of stellar origin then the absence of the characteristic absorption lines in these regions implies that the central star (perhaps a late F-type supergiant) is surrounded by an optically thick electron scattering corona. The non-stellar appearance of the nucleus and its observed polarization could probably be explained on this model.

However, it is to be noted that Thackeray (**15**) states that in the spectrum of *h* the continuum is enhanced relative to the bright lines compared with the spectrum of the nucleus. This observation is extremely difficult to reconcile with the model which assumes a stellar origin for the continuum. We conclude that Thackeray's observation, if confirmed will show that an appreciable fraction

of the continuum observed in the spectrum of condensation h is produced in h and not scattered from the nucleus.

(*c*) *The synchrotron hypothesis.* Searle *et al.* (**28**) have noted that the continuum of η Carinae shows striking similarity to that of the nucleus of the Seyfert galaxy NGC 4151. Further, the red component appears to be common to such diverse objects as the Crab nebula and the quasi-stellar radio source 3C48. One feature that these quite dissimilar objects share is that, judged by the width of the emission lines, they possess internal motions as large as a few thousand km/s. These similarities suggest an alternative explanation for the origin of the optical continuum radiation, namely that it is of synchrotron origin.

If the similarity of the spectra of η Carinae and the Crab nebulae extended to radio wavelengths then obviously η Carinae would be an extremely bright radio source. The Crab nebula is fainter by a factor of 8×10^{-3} at optical frequencies. However η Carinae is certainly not a strong radio source. Mr A. E. Le Marne of the Molonglo Radio Observatory observed the region of η Carinae at 408 Mc/s with the E–W beam of the Mills Cross. He found an upper limit to the flux of an object at the right ascension of η Carinae to be 4·5 flux units. Mr Maston Beard and Dr F. J. Kerr also observed the region of η Carinae at wavelengths of 11 and 20 cm with the Parkes 210 ft radio telescope and placed upper limits of 2·5 and 6 flux units respectively on the brightness of η Carinae*. We are very much indebted to these gentlemen for giving us permission to quote their results prior to publication. The question raised therefore is whether there is a mechanism capable of accounting for a low frequency cut-off in the hypothesized synchrotron spectrum of η Carinae.

Possible mechanisms for the attenuation of low frequency radiation in radio sources have been discussed by, *inter alia*, Hornby & Williams (**29**). With the parameters we have determined and with plausible magnetic fields ($1 > B > 10^{-6}$ gauss) the relevant possibilities are free–free absorption and the Tsytovich effect. At 11 cm a medium with an electron density of $3 \times 10^6/\text{cm}^3$ at a temperature of 2×10^4 °K and a path length of 5×10^{16} cm has an optical thickness of 2×10^3. If the energy spectrum of the relativistic particles is the same in η Carinae as in the Crab nebula then we find that an optical depth of 4×10^4 at 11 cm wavelength would be required to give the observed limit to the ratio of the radio and optical fluxes. Free–free absorption is therefore inadequate to explain the observations. On the other hand the Tsytovich effect could suppress the 11 cm flux below the observed limit of $N_e/B > 5 \times 10^8$, or with the derived density, if $B < 6 \times 10^{-3}$ gauss.

To reconcile the observed spectrum with the synchroton hypothesis we conclude it is necessary to assume that the magnetic field is less than 6×10^{-3} gauss. With $B = 6 \times 10^{-3}$ we find that the magnetic energy contained in the object is 3×10^{44} erg while the energy contained in the relativistic electrons is 2×10^{48} erg. The lifetime of electrons responsible for optical radiation is in these circumstances about one year. It is impossible to adjust the magnetic field strength to obtain a closer approach to equipartition without violating the observed data. The problems associated with the imbalance of the particle and field energy densities and the lifetime of the relativistic particles compared with th

* Since this paper was submitted for publication Mr Beard and Dr Kerr have revised the upper limit of the flux of η Carinae at 11 cm to be 10 flux units. The revision does not affect the conclusions from the discussion of Section 5 (*c*).

age of the object are of the same kind as, but more serious than, those found in the case of the Crab nebula (**30**).

There are difficulties associated with both proposals for the origin of the optical continuum in η Carinae. The matter cannot be decided with the observations that have so far been made. Quantitative spectrophotometry of the halo is much needed and observations of the object in the submillimetre range are likely to prove decisive.

Acknowledgments. We are grateful to Misses Carmel Read and Miriam Gottlieb for their assistance in the reductions of our data and Dr F. J. Kerr and Messrs Maston Beard and A. E. Le Marne for their generous provision of data prior to publication. We are also indebted to Dr N. Visvanathan for allowing us continued access to his polarization data and for the stimulating discussions raised thereby.

Mount Stromlo Observatory,
Australian National University,
Canberra, A.C.T.,
Australia.

1966 *June.*

References

(1) Innes, R. T. A., 1903. *Ann. R. Obs. Cape Town*, **IX**, 75B.
(2) O'Connell, D. J. K., 1956. *Vistas in Astronomy*, Vol. 2, p. 1165.
(3) Thackeray, A. D., 1953. *Mon. Not. R. astr. Soc.*, **113**, 211.
(4) Thackeray, A. D., 1962. *Mon. Not. R. astr. Soc.*, **124**, 251.
(5) Gaviola, E., 1953. *Astrophys. J.*, **118**, 234.
(6) Merrill, P. W., 1928. *Astrophys. J.*, **67**, 391.
(7) Gaviola, E., 1950. *Astrophys. J.*, **111**, 408.
(8) Thackeray, A. D., 1953. *Mon. Not. R. astr. Soc.*, **113**, 238.
(9) Visvanathan, N., 1966. *Mon. Not. R. astr. Soc.*, **135**, 275.
(10) Oke, J. B., 1964. *Astrophys. J.*, **140**, 690.
(11) Code, A. D., 1960. *Stellar Atmospheres* (ed. by Greenstein), p. 50. Chicago University Press.
(12) Feinstein, A., 1963. *Publs astr. Soc. Pacif.*, **75**, 492.
(13) Herschel, J., 1843. *Results of Observation at the Cape.*
(14) Hoffleit, D., 1956. *Astrophys. J.*, **124**, 61.
(15) Thackeray, A. D., 1956. *Observatory*, **76**, 103.
(16) Gratton, L., 1963. *Stellar Evolution*, Vol. 28, p. 297. Academic Press, New York.
(17) Burgess A., 1958. *Mon. Not. R. astr. Soc.*, **118**, 477.
(18) Faulkner, D. J., 1963. *Publs astr. Soc., Pacif.*, **75**, 296.
(19) Faulkner, D. J. & Aller, L. H., 1965. *Mon. Not. R. astr. Soc.*, **130**, 393.
(20) Johnson, H. L., 1965. *Astrophys. J.*, **141**, 923.
(21) House, L., 1964. *Astrophys. J. Suppl. Ser.*, **8**, 307.
(22) Parker, R. A. R., 1964. *Astrophys. J.*, **139**, 208.
(23) Seaton, M. J., 1954. *Mon. Not. R. astr. Soc.*, **114**, 154.
(24) Seaton, M. J., 1958. *Rev. mod. Phys.*, **30**, 979.
(25) Aller, L. H., 1960. *Stellar Atmospheres* (ed. by Greenstein), p. 156. Chicago University Press.
(26) Capriotti, E. R., 1964. *Astrophys. J.*, **139**, 225.
(27) Seaton, M. J., 1960. *Rep. Prog. Phys.*, **23**, 313.
(28) Searle, L., Rodgers, A. W., Sargent, W. L. W. & Oke, J. B., 1965. *Nature, Lond.*, **208**, 1190.
(29) Hornby, J. M. & Williams, P. J. S., 1966. *Mon. Not. R. astr. Soc.*, **131**, 237.
(30) Woltjer, J., 1958. *Bull. astr. Insts Neth.*, **14**, 40.